Since January 2020 Elsevier has created a COVID-19 resource centre with free information in English and Mandarin on the novel coronavirus COVID-19. The COVID-19 resource centre is hosted on Elsevier Connect, the company's public news and information website.

Sensors & Actuators: B. Chemical 327 (2021) 128899

Contents lists available at ScienceDirect

Sensors and Actuators: B. Chemical

journal homepage: www.elsevier.com/locate/snb

Ultrasensitive supersandwich-type electrochemical sensor for SARS-CoV-2 from the infected COVID-19 patients using a smartphone

Hui Zhao [a,1], Feng Liu [a,1], Wei Xie [a,1], Tai-Cheng Zhou [b,1], Jun OuYang [a], Lian Jin [a], Hui Li [b], Chun-Yan Zhao [b], Liang Zhang [b], Jia Wei [b,*], Ya-Ping Zhang [a,c,*], Can-Peng Li [d,**]

[a] State Key Laboratory for Conservation and Utilization of Bio-Resources in Yunnan, School of Life Sciences, Yunnan University, Kunming, 650091, China
[b] Central Lab, Liver Disease Research Center, the Second People's Hospital of Yunnan Province, Kunming, 650021, China
[c] State Key Laboratory of Genetic Resources and Evolution, Kunming Institute of Zoology, Chinese Academy of Sciences, Kunming, 650223, China
[d] School of Chemical Science and Technology, Yunnan University, Kunming, 650091, China

ARTICLE INFO

Keywords:
SARS-CoV-2
Electrochemical biosensor
Supersandwich-type biosensor
Smartphone
Calixarene

ABSTRACT

The recent pandemic outbreak of COVID-19 caused by a novel severe acute respiratory syndrome coronavirus 2 (SARS-CoV-2), poses a threat to public health globally. Thus, developing a rapid, accurate, and easy-to-implement diagnostic system for SARS-CoV-2 is crucial for controlling infection sources and monitoring illness progression. Here, we reported an ultrasensitive electrochemical detection technology using calixarene functionalized graphene oxide for targeting RNA of SARS-CoV-2. Based on a supersandwich-type recognition strategy, the technology was confirmed to practicably detect the RNA of SARS-CoV-2 without nucleic acid amplification and reverse-transcription by using a portable electrochemical smartphone. The biosensor showed high specificity and selectivity during *in silico* analysis and actual testing. A total of 88 RNA extracts from 25 SARS-CoV-2-confirmed patients and eight recovery patients were detected using the biosensor. The detectable ratios (85.5 % and 46.2 %) were higher than those obtained using RT-qPCR (56.5 % and 7.7 %). The limit of detection (LOD) of the clinical specimen was 200 copies/mL, which is the lowest LOD among the published RNA measurement of SARS-CoV-2 to date. Additionally, only two copies (10 μL) of SARS-CoV-2 were required for per assay. Therefore, we developed an ultrasensitive, accurate, and convenient assay for SARS-CoV-2 detection, providing a potential method for point-of-care testing.

1. Introduction

The coronavirus disease 2019 (COVID-19) is a novel emerging human infectious disease caused by severe acute respiratory syndrome coronavirus 2 (SARS-CoV-2) [1,2]. As human-to-human transmission rapidly increased, COVID-19 has spread globally and poses a threat to public health in more than 200 countries. On March 11, 2020, the World Health Organization (WHO) classified the COVID-19 outbreak as a pandemic [3]. As of 4 Sep 2020, more than 26,495,880 cases of COVID-19 have been confirmed around the world, resulting in 873,618 deaths [4]. Hence, early and accurate diagnostics is undoubtedly of vital importance to the containment of COVID-19 because it facilitates the control of infection sources and monitoring of illness progression.

Given that COVID-19 patients have nonspecific symptoms, SARS-CoV-2 detection is indispensable in accurate diagnosis. SARS-CoV-2 is a novel coronaviridae virus possessing a single-strand and positive RNA genome with ~3 kb length [5]. The genome comprises a 5′ untranslated region (UTR), replicase complex (ORF1ab), spike surface glycoprotein gene (S gene), small envelope gene (E gene), matrix gene (M gene), nucleocapsid gene (N gene), 3′UTR, and several unidentified non-structural open reading frames [5]. Although antibody-based serological test is rapid and convenient, the shortcomings of the technology limit its applicability. For example, generating an antibody against SARS-CoV-2 following symptom onset for detection takes a substantial amount of time. SARS-CoV-2 antibodies have potential cross-reactivity with antibodies generated against other coronaviruses. Therefore, nucleic acid-based real-time reverse transcription PCR (RT-qPCR) assays are globally utilized as a golden standard for virus

* Corresponding authors.
** Corresponding author at: School of Chemical Science and Technology, Yunnan University, Kunming, 650091, China
E-mail addresses: weijia19631225@163.com (J. Wei), zhangyp@mail.kiz.ac.cn (Y.-P. Zhang), lcppp1974@sina.com (C.-P. Li).
[1] These authors contributed equally to this work.

https://doi.org/10.1016/j.snb.2020.128899
Received 21 July 2020; Received in revised form 5 September 2020; Accepted 10 September 2020
Available online 14 September 2020

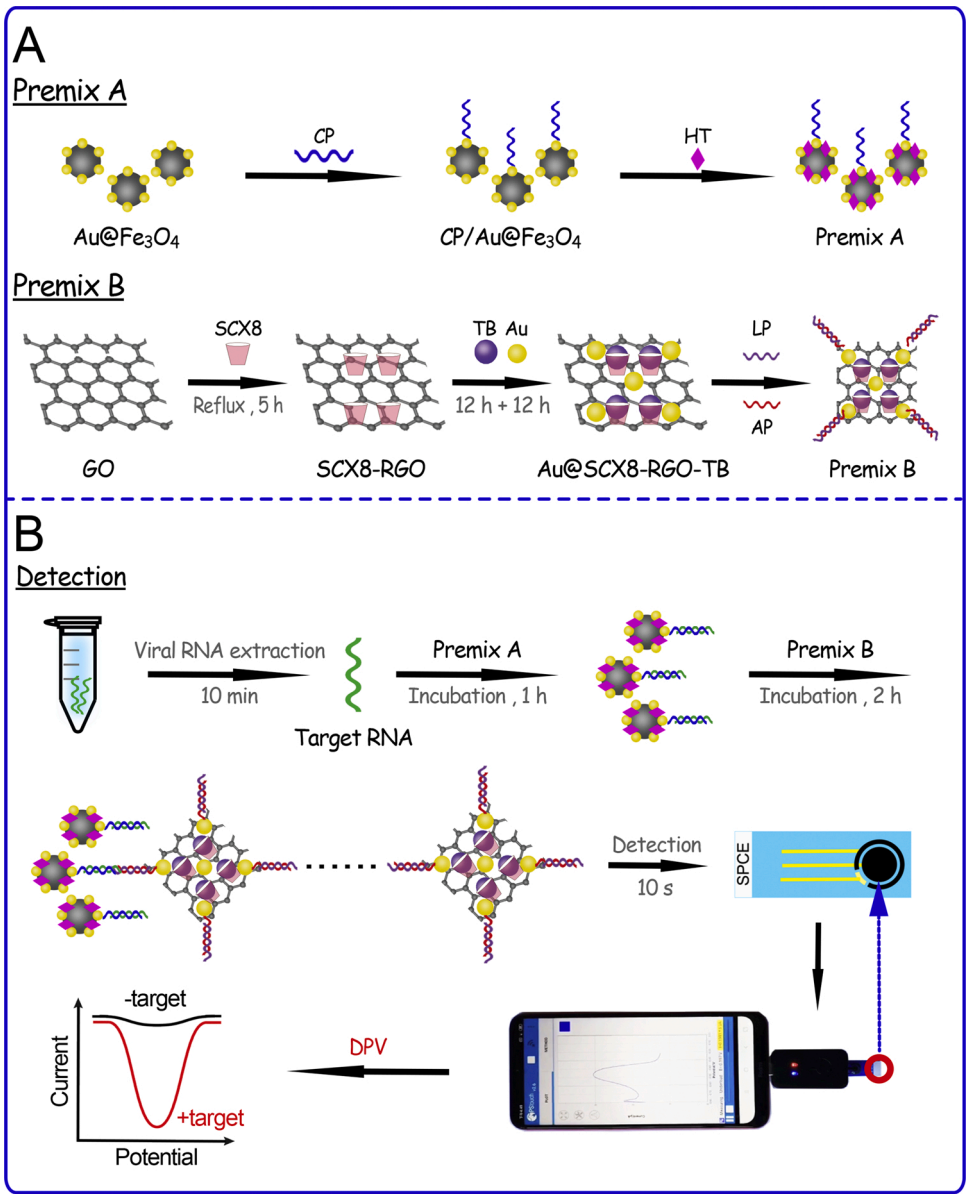

Scheme 1. Schematic representation of SARS-CoV-2 detection using the electrochemical biosensor. (A) Prepare of premix A and B; (B) Process of electrochemical detection using a smartphone.

RNA detection. However, RT-qPCR has some drawbacks, such as expensive instruments and reagents, and need for trained personnel, and thus specimens need to be shipped to reference laboratories. Currently, 11 nucleic-acid-based RT-qPCR detection kits have been approved by the China National Medical Products Administration (NMPA) for SARS-CoV-2 diagnostics [6]. False-negative results as high as 20%–40% have been reported in China [7]. These results may be attributed to various factors, including sample source and quality, personnel operation, and test kit sensitivity. Undisputedly, detectable sensitivity is a crucial issue for the accurate diagnosis of COVID-19. According to the report by Wang et al. [8], six commercial RT-qPCR kits approved by the China NMPA have poor limits of detection (LODs) and likely lead to false-negative results. Therefore, developing accurate and easy-to-implement methods for COVID-19 detection is necessary.

Electrochemical biosensors provide an alternative and reliable solution to clinical diagnosis due to their advantages, such as high sensitivity, low cost, user-friendliness, and robustness [9]. Especially, with the miniaturization and intelligent development of electrochemical device, electrochemical biosensors are considered useful in clinical diagnosis and point-of-care testing (POCT). In the field of nucleic acid biosensors, a supersandwich-type electrochemical biosensor has attracted considerable attention due to their high specificity and sensitivity [10]. This type of biosensor is composed of capture probe (CP), target sequence, label probe (LP), and auxiliary probe (AP) [11]. The 5′- and 3′-terminals of target sequence are complementary to CP and LP, respectively, and the 5′- and 3′-regions of AP have complementary sequences with two different LP areas [11,12]. Therefore, sequence-specific detection can be achieved by using CP and LP, and AP hybridizes many times with LP to produce long concatamers, resulting in high sensitivity. However, in a traditional supersandwich-type electrochemical biosensor, each LP was labeled only one signal molecule and resulted low current signal. Therefore, we hypothesized that the sensitivity of the biosensor can be improved by facilitating of LP with signal molecules through other molecules or materials.

Host-guest recognition has attracted attention in the fabrication of electrochemical biosensors. Given that host-guest recognition motifs are specific and biorthogonal, they can form stable host-guest inclusion to increase the enrichment capability of guest molecules due to own more

Table 1
Sequences of artificial target, probes, and RT-qPCR primers used in this study.

For ORF1ab detection	5′ → 3′
Target ssDNA	CCCTGTGGGTTTTACACTTAAAAACACAGTCTGTACCGTCTGCGGTATGTG GAAAGGTTATGGCTGTAGTTGTGATCAACTCCGCGAACCCATGCTTCAGT CAGCTGATGCACAATCGT
Capture probe (CP)	ACCTTTCCACATACCGCAGACG-$(CH_2)_6$-SH
Labeled signal probe (LP)	TCGAGTTACGCTAAGCGCGGAGTTGATCACAACTA-$(CH_2)_6$-SH
Auxiliary probe (AP)	CTTAGCGTAACTCGATAGTTGTGATCAACTCCGCG
Single-base mismatch target (1 M T)	CGTCTGCGGTACGTGGAAAGGTTATGGCTGTAGTTGTGATCAACTCCGCG
Two-base mismatch target (2 M T)	CGTCTGCGGTACATGGAAAGGTTATGGCTGTAGTTGTGATCAACTCCGCG
RT-qPCR primer	5′ → 3′
ORF1ab_F	CCCTGTGGGTTTTACACTTAA
ORF1ab_R	ACGATTGTGCATCAGCTGA

rigid and well-defined cavity [13–15]. Interesting macrocyclic host molecules, calixarenes, such as CX8, show excellent supramolecular recognition and enrichment capability for the electrochemical mediators of methylene blue and toluidine blue (TB) [16–19]. Additionally, Au metal nanoparticles (NPs) have been widely used in improving biosensor sensitivity due to their various advantages, such as good conductivity, large surface area, and strong adsorption capability [20]. Through the coordination of Au-S, probe functionalized sulfhydryl groups are immobilized with Au NPs anchored on material surfaces [17, 21].

In the present study, we developed a supersandwich-type electrochemical biosensor based on p-sulfocalix[8]arene (SCX8) functionalized graphene (SCX8-RGO) to enrich TB for SARS-CoV-2 RNA detection (Scheme 1). We developed a plug-and-play method to achieve the sensitive, accurate, and rapid detection of SARS-CoV-2 samples from various clinical specimens without RNA amplification using an electrochemical biosensor equipped with a smartphone, providing a simple, low-cost and useful method for POCT.

2. Materials and methods

2.1. Chemicals and materials

Graphite oxide was purchased from Nanjing XFNANO Materials Tech Co., Ltd (Nanjing, China). SCX8 was obtained from Tokyo Chemical Industry Co., Ltd (Tokyo, Japan). A Carbon-Three Electrode screen printing carbon electrode (SPCE) was purchased from Zensor Research & Development Co., Ltd (Beijing, China). TB was obtained from Aladdin Industrial Corporation (Shanghai, China). All the reagents were of analytical grade. All the aqueous solutions were prepared with diethyl pyrocarbonate, and the effect of RNAase on the mRNA stability was minimized by autoclaving all the sample tubes and glassware.

2.2. Apparatus

Differential pulse voltammetry (DPV) was performed with a smartphone equipped with a Sensit Smart electrochemical workstation from Palmsens (Netherlands). The morphologies of the prepared samples were characterized by JEM 2100 transmission electron microscopy (TEM, Tokyo, Japan). A Thermo Fisher Scientific Nicolet IS10 Fourier transform infrared (FTIR, Waltham, USA) Impact 410 spectrophotometer and a Q50 thermogravimetric analysis (TGA) instrument (New Castle, USA) were used for the FTIR study and TGA analysis, respectively. An ESCALAB 250 photoelectron spectrometer (Thermo-VG Scientific, USA) was used for X-ray photoelectron spectroscopy (XPS) analysis. A Bruker D8-advance X-ray diffractometer (Germany) was carried out X-ray powder diffraction (XRD) experiment. A Malvern Zetasizer Nano (Malvern, England) electrochemical workstation was used for the zeta potential measurements. QuantStudio 5 Real-Time PCR System (Thermo Fisher Scientific, MA, USA) was used for qPCR experiment.

2.3. Probe and primer design

Primer pairs were synthesized according to the sequences provided by the Chinese Center for Disease Control and Prevention (CDC) and used to amplify ORF1ab gene in real-time PCR (qPCR). The sequences of CPs to ORF1ab gene were selected from the above PCR amplicon sequences. The sequences of the designed probes and primers are summarized in Table 1. The primers and probes were synthesized by Tsingke Biotechnology (Beijing, China). In specificity analysis, we aligned the complete genomes of SARS-CoV-2 through the BLAST analysis of NCBI COVID resources (https://blast.ncbi.nlm.nih.gov/Blast.cgi), and then a high conservation region was selected. The blast analyses were further performed using the genomes of the 39 respiratory pathogens listed in Table S1.

2.4. Preparation of premixes A and B for SARS-CoV-2 detection

For premix A preparation, Fe_3O_4 NPs were prepared and dissolved, and then PEG400, trisodium citrate, $HAuCl_4$, and ascorbic acid were successively added for the production of Au@Fe_3O_4 nanocomposite. Then, 100 μL of 1 mg mL^{-1} Au@Fe_3O_4 dissolved in Buffer I (10 mM Tris-HCl containing 1 mM EDTA, 300 mM NaCl, and 10 mM TCEP, pH7.4) was incubated with 10 μL of 1 μM CP at 4 °C for 12 h. For the eliminate of non-specific binding, 10 μL of 1 mM hexane-1-thiol (HT) was added to the above mixture at room temperature for half an hour. Lastly, the precipitation was dissolved with 100 μL of Buffer II (10 mM Tris-HCl containing 1 mM EDTA, 300 mM NaCl, and 1 mM $MgCl_2$, pH 7.4) and mixed slowly at 4 °C for 12 h.

For premix B preparation, graphene oxide (GO) and SCX8 aqueous solution were dissolved through sonication and refluxed. Then, $HAuCl_4$ and TB solution were successively added for the production of Au@SCX8-RGO-TB nanocomposites. Next, 100 μL of 1 mg mL^{-1} Au@SCX8-RGO-TB dissolved in Buffer I was incubated with 10 μL of 1 μM LP at 4 °C for 12 h. After the supernatant was removed, the precipitate was added to 10 μL of 1 μM AP and 90 μL of Buffer II, and the resulting mixture was stored at room temperature before use.

2.5. Preparation of detection samples

Detection samples included artificial targets and clinical RNA samples. The sequences of artificial targets are listed in Table 1. Given that RNA is easy to degrade, we synthesized the corresponding target sequences of single-strand DNA (ssDNA) according to the published RNA sequences of SARS-CoV-2 (GenBank No. MN908947.3) for electrochemical detection. The annealed sequences were cloned to a pUC57 plasmid for copy number calculation.

All the clinical specimens used in this study were collected from the Second People's Hospital of Yunnan Province and approved by the Ethical Committee of the Second People's Hospital of Yunnan Province. Patients with COVID-19 were confirmed by CT scans and nucleic acid testing according to the Chinese CDC guideline [22]. A total of 88

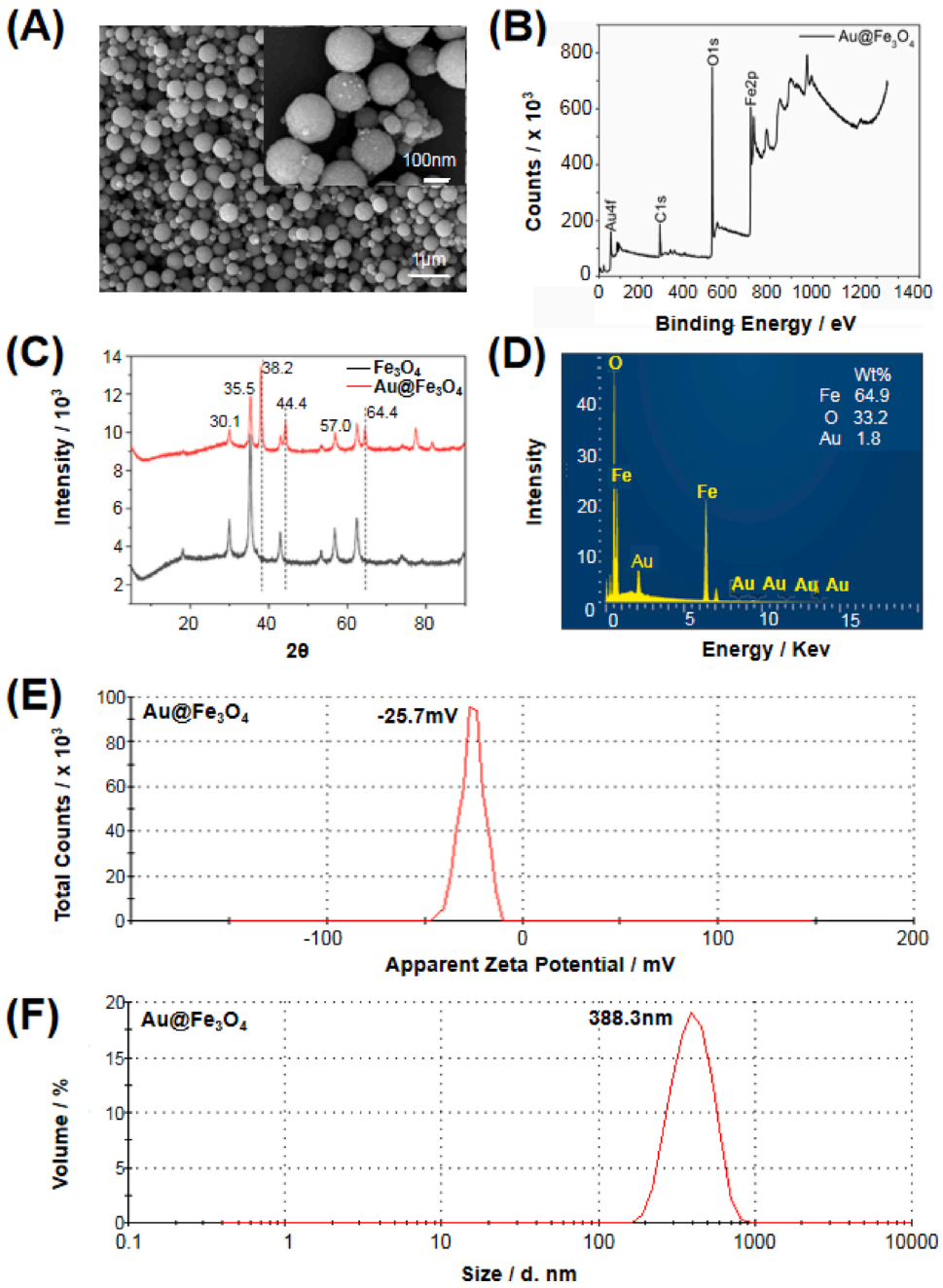

Fig. 1. (A) SEM image of $Au@Fe_3O_4$; (B) XPS patterns of $Au@Fe_3O_4$; (C) XRD patterns of Fe_3O_4 and $Au@Fe_3O_4$; (D) EDS patterns of $Au@Fe_3O_4$; (E) Zeta Potential patterns of $Au@Fe_3O_4$; (F) The diameter of $Au@Fe_3O_4$.

samples from 25 confirmed patients and eight recovery patients infected by SARS-CoV-2 were collected and inactivated by heating at 56 °C for 30 min. A total of 24 respiratory pathogens were used for specific analysis, including three samples from influenza A virus, six samples from influenza B virus, one sample from parainfluenza virus, one sample from adenovirus, 10 samples from *Mycoplasma pneumonia*, one sample from *Klebsiella pneumoniae*, one sample from *Chlamydia pneumonia*, and one sample from *Legionella pneumophila*. Total RNAs were extracted using a Tianlong DNA/RNA virus mini-kit (Tianlong, Xi'an, China). The quantities and quality of the extracted RNAs were spectrophotometrically assessed using NanoDrop 2000 (Thermo Scientific). The prepared samples were stored at −80 °C before use.

2.6. Electrochemical measurement

The mixture of 50 μL of premix A and 10 μL of detection samples were incubated for 1 h, and the supernatant was removed through magnetic separation. Then, 50 μL of premix B was added to the sediment and incubated for 2 h. The supernatant was removed by magnetic separation and washed with PBS (pH 7.2) three times. Finally, the resulting nanocomposite was dissolved in 50 μL of PBS and dropped on SPCE for electrochemical measurement. All the reactions were performed at room temperature.

2.7. RT-qPCR measurement

The measurements of SARS-CoV-2 were performed using a commercial 2019-nCOV ORF1ab/N nucleic acid detection kit (Tianlong,

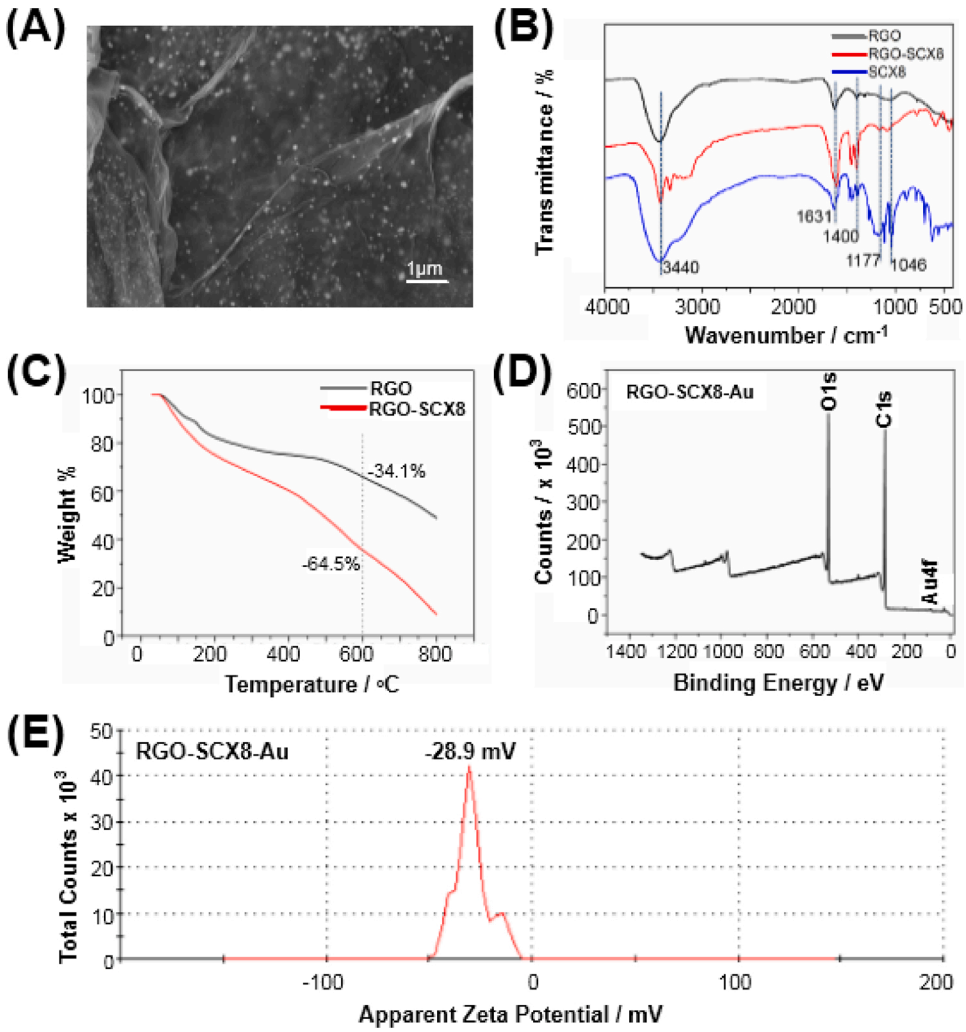

Fig. 2. (A) SEM image of RGO-SCX8-Au; (B) FT-IR spectra of SCX8, RGO and RGO-SCX8; (C) TGA curves of RGO and RGO-SCX8; (D) XPS patterns of RGO-SCX8-Au; (E) Zeta Potential patterns of RGO-SCX8-Au.

Xi'an, China). The reaction was set up according to the manufacturer's protocol. ORF1ab or N genes with a cycle threshold (Ct value) of <37 was considered positive samples. The copy number concentration of the plasmid with the ORF1ab fragment was calculated using the following formula: copies/mL = $6.02 \times 10^{23} \times 10^{-6} \times$ concentration (ng/μL)/(fragment length × 660). Then, the 10-fold serial dilutions of the plasmid ranged from 10^3 to 10^9 copies/mL and subjected to qPCR. A standard curve was obtained.

2.8. Statistical analysis

Fisher's exact test was used in comparing the performance of the assays with SPSS 22.0 (IBM). A p-value of <0.05 was considered statistically significant and indicated that the sample is a positive sample.

3. Results and discussion

3.1. Characterization of nanocomposites

For the characterization of Au@Fe_3O_4 particles, the morphology and microstructure of Au@Fe_3O_4 were analyzed through SEM. As shown in Fig. 1A, Fe_3O_4 nanoparticles were spherical and had smooth surfaces, and Au nanoparticles were anchored on the Fe_3O_4 surface. Furthermore, the elemental analysis of Au@Fe_3O_4 demonstrated the presence of Fe, O, and Au in the composite nanohybrids through XPS (Fig. 1B). Compared with the XRD patterns of Fe_3O_4, the XRD patterns of Au@Fe_3O_4 showed special characteristics at 38.2°, 44.4°, and 64.6° (Fig. 1C), and the EDS result showed that the contents of Fe, O, and Au in the Au@Fe_3O_4 composite material were 64.9 %, 33.2 %, and 1.8 %, respectively (Fig. 1D). As shown in Fig. 1E, Au@Fe_3O_4 was negative-charged, which was attribute to the Au NPs on the Fe_3O_4 surface. The average particle size of Au@Fe_3O_4 was approximately ~388.3 nm (Fig. 1F). All the results confirmed the successful loading of Au-NPs with Fe_3O_4.

The morphology of the RGO-SCX8-Au composite material was investigated through SEM, RGO-SCX8-Au was a single-layer sheet structure, and Au NPs were evenly distributed on its surface (Fig. 2A). As shown in Fig. 2B, the FTIR spectrum revealed a stretching vibration of −OH (3440 cm^{-1}), an oxygen-containing functional group C—O/C-C (1046 cm^{-1}), and a conjugate C═C (1631 cm^{-1}) in RGO material, and the peak vibration of −OH (3440 cm^{-1}) and O—H bending (1400 cm^{-1}) significantly enhanced in the RGO-SCX8 composite. Furthermore, the characteristic peak of CH_2 (3190 cm^{-1}) and typical peaks of -SO_3- at 1177 cm^{-1} were observed in the RGO-SCX8 composite, suggesting that SCX8 was successfully grafted onto the RGO. The TGA result showed that the lost mass of RGO was approximately 34.1 % at 600 °C. By contrast, the RGO-SCX8 material lost approximately 64.5 % mass at the same temperature (Fig. 2C). Thus, the mass loss caused by the decomposition of SCX8 was 30.4 % in the RGO-SCX8 composites, indicating that the RGO-SCX8 material was successfully prepared. The XPS patterns of RGO-SCX8-Au showed Au, C, and O were detected in the

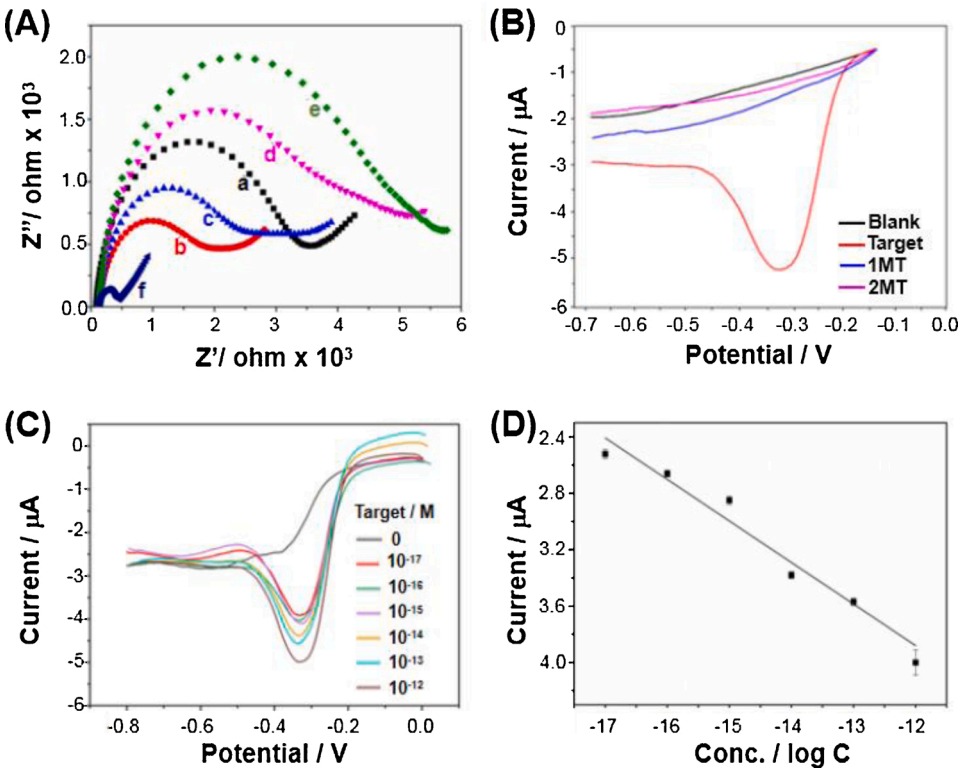

Fig. 3. The feasibility of the proposed SARS-CoV-2 biosensor. (A) EIS characterization of modified electrodes of SARS-CoV-2 biosensor in 0.1 M PBS (pH 7.2) containing 2.0 mM [Fe $(CN)_6]^{3-/4-}$ and 0.1 M KCl. (a) bare screen printing carbon electrode (SPCE); (b) Au@Fe_3O_4/SPCE; (c) CP/Au@Fe_3O_4/SPCE; (d) HT/CP/Au@Fe_3O_4/SPCE; (e) Target/HT/CP/Au@Fe_3O_4/SPCE; (f) Au@SCX8-TB-RGO-AP-LP-Target/HT/CP/ Au@Fe_3O_4. (B) DPV curves for the artificial target, one-mismatch target (1 M T) and two-mismatch target (2 M T) of 10^{-12} M. (C) DPV curves for different concentrations of artificial target for the SARS-CoV-2 biosensor. (D) The resulting calibration plot for log[C] vs. DPV response in the range of 10^{-17}-10^{-12} M.

material (Fig. 2D). As shown in Fig. 2E, the Zeta potential of the RGO-SCX8-Au composites was -28.9 mV, suggesting that the colloidal stability of RGO-SCX8-Au was well dispersed. All the above results demonstrated that the successful preparation of the RGO-SCX8-Au nanocomposites.

3.2. Fabrication of electrochemical biosensor

In this study, we designed and assembled the supersandwich-type biosensor for SARS-CoV-2 through the following procedures: i) the CPs labeled with thiol were immobilized on the surfaces of the Au@Fe_3O_4 nanoparticles and formed CP/Au@Fe_3O_4 nanocomposites; ii) the host-guest complexes (SCX8-TB) were immobilized on RGO to form Au@SCX8-TB-RGO-LP bioconjugate; iii) the sandwich structure of "CP-target-LP" produced; and iv) AP was introduced to form long concatamers (Scheme 1).

To monitor the assembling process of the modified SPCE electrode, we characterized the interface properties using electrochemical apparatus by EIS techniques. As shown in Fig. 3A, the results of the impedance spectra showed that the electron-transfer of the SPCE electrode modified by Au@Fe_3O_4 (curve b) distinctly reduced compared with the bare SPCE electrode (curve a), suggesting that the Au@Fe_3O_4 NPs were successfully attached onto the surface of electrode and resulted high conductivity. Subsequently, after the addition of CP and HT in succession, the resistance of the modified SPCE increased step by step (curves c and d) because these additives hampered electron transfer. Resistance increased (curve e) after incubation with the artificial target, because the complex formation of the Target/HT/CP/Au@Fe_3O_4 further increased the steric hindrance and hindered electron shuttle. However, the resistance of the probe nanocomposite (Au@SCX8-TB-RGO-AP-LP-Target/HT/CP/Au@Fe_3O_4) modified SPCE (curve f) sharply decreased due to the high conductivity of Au NP and RGO. The above results suggested that the proposed biosensor was successfully fabricated.

3.3. Detection of artificial target by SARS-CoV-2 biosensor

Given that COVID-19 is a person-to-person transmission disease, we synthesized the artificial target of ssDNA according to the sequences of SARS-CoV-2 RNA and explored the feasibility of the biosensor. As shown in Fig. 3B, a high electrochemical signal peak (DPV) was observed after incubation with the artificial target (10^{-12} M), and DPV signal was extremely weak in the absence of a target, suggesting that the proposed electrochemical method is feasible for SARS-CoV-2 detection. The conditions for the SARS-CoV-2 biosensor assay on the ORF1ab gene were optimized. Specifically, 50 μL of premix A and 10 μL of target samples were incubated at room temperature for 1 h, then incubated with 50 μL of premix B at room temperature for 2 h (Fig. S1). Finally, the electrochemical signal of TB was detectable in <10 s by the portable smartphone (Scheme 1). Thus, the assay was easy-to-implement and rapid.

The DPV measurements of the SARS-CoV-2 biosensor were further performed using the artificial targets under different concentrations. As shown in Fig. 3C, DPV peaks were enhanced with the increase of the artificial targets concentration, indicating a clear dependence on target concentration. The resulting calibration plot presented a good line relationship between current and the logarithm concentrations of the artificial targets (ranging from 10^{-17} to 10^{-12} M with an LOD of 3 aM; Fig. 3D). The corresponding regression equation was calculated as I (μA) $= -0.295\log C - 7.416$ ($R^2 = 0.945$). The proposed SARS-CoV-2 biosensor manifested high sensitivity due to the good conductivity of Au NP and RGO materials and enrichment capability of signal molecule TB based on the supramolecular recognition of SCX8.

3.4. Detection of SARS-CoV-2 from clinical samples

A total of 88 RNA samples from 25 confirmed patients and eight recovery patients who had negative RNA tests after cure and then turned RNA positive, were used in detecting SARS-CoV-2 with three replicates at each sample. These specimens included sputum (17, 19.32 %), throat swabs (20, 22.73 %), urine samples (15, 17.05 %), plasma samples (10, 11.36 %), feces samples (11, 12.50 %), oral swabs (3, 3.41 %), serum

Table 2
Comparison of the electrochemical assay with the RT-qPCR assay for detection of SARS-CoV-2 from clinical specimens.

		Positive sample / Total sample = Detection ratio	
Source	Specimens	Electrochemical method	qPCR method
Confirmed patients	Sputum	11/11 = 100 %	10/11 = 90.9 %
	Throat swab	15/17 = 88.2 %	12/17 = 70.59 %
	Urine	8/10 = 80 %	2/10 = 20 %
	Feces	6/6 = 100 %	3/6 = 50 %
	Plasma	8/9 = 88.9 %	4/9 = 44.4 %
	Serum	2/5 = 40 %	2/5 = 40 %
	Whole blood	1/1 = 100 %	0/1 = 0
	Oral swab	1/2 = 50 %	1/2 = 50 %
	Saliva	1/1 = 100 %	1/1 = 100 %
	Total	53/62 = 85.5 %	35/62 = 56.5 %
Recovery patients	Sputum	4/6 = 66.7 %	2/6 = 33.3 %
	Throat swab	1/3 = 33.3 %	0/3 = 0
	Urine	2/5 = 40 %	0/5 = 0
	Feces	1/5 = 20 %	0/5 = 0
	Plasma	1/1 = 100 %	0/1 = 0
	Serum	1/3 = 33.3 %	0/3 = 0
	Whole blood	1/2 = 50 %	0/2 = 0
	Oral swab	1/1 = 100 %	0/1 = 0
	Total	12/26 = 46.2 %	2/26 = 7.7 %

samples (8, 9.09 %), whole blood samples (3, 3.41 %), and saliva sample (1, 1.14 %). To compare the sensitivity of the proposed biosensor, we carried out the RT-qPCR method, using the same RNA extraction from the above specimens. The RT-qPCR results showed that 35 samples were positive in 62 samples from the confirmed patients (56.5 %), and two from 26 samples from the recovery patients (7.7 %) were present (Table 2). Similar positive ratio of nucleic acid detection for SARS-CoV-2 was detected in other Chinese groups through RT-qPCR [7,23]. Notably, the electrochemical detection results of the 34 of the 35 positive samples were positive. However, 19 negative samples identified by RT-qPCR were positive according to electrochemical detection. Consequently, the detectable positive rate achieved 85.5 % and 46.2 % in the confirmed and recover patients by the proposed SARS-CoV-2 biosensor, respectively, demonstrating that electrochemical assay is more sensitive than RT-qPCR assay for SARS-CoV-2 determination.

The respiratory samples used for diagnosing COVID-19 were divided into upper respiratory samples (throat swab, oral swab, and oropharyngeal swab) and lower respiratory samples (e.g. sputum). In accordance with other studies [24,25], our results showed the sputum of lower respiratory sample was a reliable sample source for SARS-CoV-2 detection attributed to high viral load (11/11 for biosensor detection and 10/11 for RT-qPCR assay; Table 2). However, upper respiratory samples were broadly recommended for diagnosis because lower respiratory samples, especially for bronchoalveolar fluid and tracheal aspirates, have a high risk for aerosol generation [26]. Therefore, developing a sensitive detection method for samples with a low viral load is of vital importance. Interestingly, compared with to RT-qPCR assay, our SARS-CoV-2 biosensor was superior to other assay in the detection of upper respiratory samples and other low-viral-load samples from feces, urine, and plasma (Table 2).

To investigate detectable sensitivity, we analyzed the LODs of clinical specimens with the SARS-CoV-2 biosensor. First, the concentrations of viral RNAs extracted from throat swabs were measured in copies per milliliter. The resulting calibration plot for log(copy numbers) vs. Ct values (Fig. S2) was used. Then, the diluted viral RNA samples were detected 10 times with the SARS-CoV-2 biosensor for each concentration. Finally, the lowest concentration level with a detection rate of 100 % for positive results was regarded as the LOD of the SARS-CoV-2 biosensor. Consequently, the LOD of the proposed SARS-CoV-2 biosensor was confirmed to be 200 copies/mL (Table S2). Other published assays for SARS-CoV-2 detection are listed in Table 3. Intriguingly to the best of our knowledge, our method has the lowest LOD and required the lowest number of copies per assay, providing an ultrasensitive assay. The proposed SARS-CoV-2 biosensor presented high sensitivity and specificity due to the following factors: i) the use of the supersandwich-type electrochemical biosensor improved binding specificity and increased signal enrichment ability; ii) several nanomaterials of high conductivity promoted signal intensity; and iii) the supermolecular recognition played an important role in the enrichment of electroactive molecule TB for improving sensitivity of the biosensor.

3.5. Selectivity and specificity of the biosensor

To ensure detection accuracy, we initially performed homology analyses of our designed CP sequences targeting SARS-CoV-2 *in silico*. After the alignment of 2291 the complete genomes of SARS-CoV-2 obtained from GenBank databases, the results showed the SARS-CoV-2 RNA sequences binding to CP were completely conserved (100 %). A similar result was obtained by Wang et al. [27]. Selectivity test was performed on an artificial one-mismatch target (1 M T) and two-mismatch target (2 M T) with the SARS-CoV-2 biosensor. Compared with the distinct current peak in the presence of the artificial target, the response was hardly detected incubation with 1 M T, 2 M T, or PBS (blank), respectively (Fig. 3B).

No significant similarity was found in the genome sequences of the other 39 human respiratory pathogens *through in silico* analysis,

Table 3
Comparison of different methods for SARS-CoV-2 RNA determination.

Method/ manufacturer		Target	LOD (copies/mL)	RNA Volume (μL)	Copies per assay	Reference
RT-qPCR	Invitrogen	RdRP	760	5	3.8	[28]
		E	1040	5	5.2	
		N	1660	5	8.3	
	ThermoFisher	ORF1b/N	2500	4	10	[29]
	Liferiver	ORF1ab/N/E	484	5	2.4	[8]
	Huada	ORF1ab	484	10	4.8	
	GeneoDx	ORF1ab/N	7744	2	15.5	
	DAAN	ORF1ab/N	484	5	2.4	
	Sansure	ORF1ab/N	484	10	4.9	
	BioGerm	ORF1ab/N	986	5	4.9	
DETECTR		E/N	1000	10	10	[30]
RealStar® SARS-CoV-2		E/S	1200	10	12	
ePlex® SARS-CoV-2		N	600	200	120	[31]
COVID-19 RT-PCR panel		N	1200	5	6	
Simplexa™ COVID-19		S/ORF1ab	1584	5	7.9	[32]
RT-LAMP		N	1.31×10^5	3	393	[33]
QIAstat-SARS		E	1000	5	5	[34]
Electrochemical biosensor		ORF1ab	200	10	2	Our work

including SARS-CoV, MERS-CoV, HCoV−OC43, and influenza A, and so on (Table S1). Furthermore, the SARS-CoV-2 biosensor detected 27 clinical samples infected by influenza A virus (n = 3), Epstein-Barr virus (n = 1), *Mycoplasma pneumoniae* (n = 10), *Chlamydia pneumoniae* (n = 1), parainfluenza virus (n = 1), influenza B virus (n = 6), adenovirus (n = 1), Klebsiella pneumonia (n = 1), Candida albicans (n = 1), yeast-like fungal spores (n = 1), and *Legionella pneumophila* (n = 1). No significant electrochemical signal was found for the RNA extractions (data not shown), suggesting that no cross-reactivity for other respiratory pathogens occurred by SARS-CoV-2 biosensor. These results indicated that the proposed biosensor can accurately detect SARS-CoV-2 because of its high specificity and selectivity.

To the best of our knowledge, this work is the first to report the electrochemical detection of SARS-CoV-2 with a smartphone. Notably, the method does not require nucleic acid amplification and reverse transcription, samples are not needed to be transferred to laboratories, and no large-scale instrument and educated analysts are required. Thus, our proposed technology is a novel and plug-and-play diagnostic system, and the near-POC test remedies the shortcomings of PCR-based RNA assays. The future development of this technology is to explore microfluidic-based cartridges for high-throughput diagnostics.

CRediT authorship contribution statement

Hui Zhao: Conceptualization, Data curation, Investigation, Project administration, Supervision, Validation, Writing - original draft. **Feng Liu:** Conceptualization, Project administration, Supervision, Validation. **Wei Xie:** Supervision, Validation, Writing - review & editing. **Tai-Cheng Zhou:** Supervision, Validation, Writing - review & editing. **Jun OuYang:** Project administration, Supervision, Validation. **Lian Jin:** Project administration, Supervision, Validation. **Hui Li:** Supervision, Validation. **Chun-Yan Zhao:** Project administration, Supervision, Validation. **Liang Zhang:** Project administration, Supervision, Validation. **Jia Wei:** Conceptualization, Project administration, Supervision, Validation. **Ya-Ping Zhang:** Conceptualization, Project administration, Supervision, Funding acquisition. **Can-Peng Li:** Conceptualization, Project administration, Supervision, Validation, Funding acquisition.

Declaration of Competing Interest

The authors declare that they have no conflict of interest.

Acknowledgements

This work was supported by grants of the National Natural Science Foundation of China (31760311; 21764005), Key Projects of Yunnan Natural Science Foundation (2018FA005), Key Research and Development Projects of Yunnan (2018BC005), Major Science and Technology Special Project of Yunnan Province (Biomedicine), Program for Excellent Young Talents of Yunnan University, and the Program for Donglu Scholars of Yunnan University.

Appendix A. Supplementary data

Supplementary material related to this article can be found, in the online version, at doi:https://doi.org/10.1016/j.snb.2020.128899.

References

[1] A. Wu, Y. Peng, B. Huang, X. Ding, X. Wang, P. Niu, J. Meng, Z. Zhu, Z. Zhang, J. Wang, A new coronavirus associated with human respiratory disease in China, Cell Host Microbe 27 (2020) 325.
[2] Coronaviridae Study Group of the International Committee on Taxonomy of Viruses, The species severe acute respiratory syndrome-related coronavirus: classifying 2019-nCoV and naming it SARS-CoV-2, Nat. Microbiol. 5 (2020) 536–544.
[3] Web reference 1: WHO Timeline-COVID-19, https://www.who.int/zh/news-room/detail/27-04-2020-who-timeline-covid-19 (accessed 2020/04/27).
[4] Web reference 2: COVID-19 Coronavirus Pandemic, https://www.worldometers.info/coronavirus/(accessed 2020/09/04).
[5] F. Wu, S. Zhao, B. Yu, Y.M. Chen, W. Wang, Z.G. Song, Y. Hu, Z.W. Tao, J.H. Tian, Y.Y. Pei, M.L. Yuan, Y.L. Zhang, F.H. Dai, Y. Liu, Q.M. Wang, J.J. Zheng, L. Xu, E. C. Holmes, Y.Z. Zhang, A new coronavirus associated with human respiratory disease in China, Nature 579 (2020) 265–269.
[6] Web reference 3: State Food and Drug Administration emergency approval of new coronavirus detection products, http://www.nmpa.gov.cn/WS04/CL2056/375802. html (accessed 2020/03/25).
[7] T. Ai, Z. Yang, H. Hou, C. Zhan, C. Chen, W. Lv, Q. Tao, Z. Sun, L. Xia, Correlation of chest CT and RT-PCR testing for coronavirus disease 2019 (COVID-19) in China: A report of 1014 cases, Radiology 296 (2020) E32–E40.
[8] X.L. Wang, H.P. Yao, X. Xu, P.Y. Zhang, M.M. Zhang, J.B. Shao, Y.Q. Xiao, H. L. Wang, Limits of detection of six approved RT-PCR kits for the novel SARS-coronavirus-2 (SARS-CoV-2), Clin. Chem. 66 (2020) 977–979.
[9] A.P. Turner, Biosensors: sense and sensibility, Chem. Soc. Rev. 42 (2013) 3184–3196.
[10] X.L. Zou, Y. Xiao, K.W. Plaxco, High specificity, electrochemical sandwich assays based on single aptamer sequences and suitable for the direct detection of small-molecule targets in blood and other complex matrices, J. Am. Chem. Soc. 131 (2009) 6944–6945.
[11] X. Chen, Y.H. Lin, J. Li, L.S. Lin, G.N. Chen, H.H. Yang, A simple and ultrasensitive electrochemical DNA biosensor based on DNA concatamers, Chem. Commun. 47 (2011) 12116–12118.
[12] J. Wang, A.Q. Shi, X. Fang, X.W. Han, Y.Z. Zhang, An ultrasensitive supersandwich electrochemical DNA biosensor based on gold nanoparticles decorated reduced graphene oxide, Anal. Biochem. 469 (2015) 71–75.
[13] D.A. Uhlenheuer, L. K.Petkau, Brunsveld, Combining supramolecular chemistry with biology, Chem. Soc. Rev. 39 (2010) 2817–2826.
[14] Z.Z. Yang, Y. Chen, G. Li, Z.M. Tian, L. Zhao, X. Wu, Q. Ma, M.Z. Liu, P. Yang, Supramolecular recognition of three way junction DNA by a cationic calix[3] carbazole, Chem. Eur. J. 24 (2018) 6087–6093.
[15] G. Li, X.Y. Song, H. Yu, C. Hu, M.Z. Liu, J. Cai, L. Zhao, Y. Chen, P. Yang, Supramolecular recognition of A-tracts DNA by calix[4]carbazole, Sens. Actuators B Chem. 259 (2018) 177–182.
[16] R.N. Dsouza, U. Pischel, W.M. Nau, Fluorescent dyes and their supramolecular host/guest complexes with macrocycles in aqueous solution, Chem. Rev. 111 (2011) 7941–7980.
[17] H. Zhao, L. Yang, Y.C. Li, X. Ran, H.Z. Ye, G.F. Zhao, Y.Q. Zhang, C.P. Li, A comparison study of macrocyclic hosts functionalized reduced graphene oxide for electrochemical recognition of tadalafil, Biosens. Bioelectron. 89 (2017) 361–369.
[18] L. Yang, H. Zhao, Y.C. Li, X. Ran, G.G. Deng, X.G. Xie, C.P. Li, Fluorescent detection of tadalafil based on competitive host-guest interaction using p-sulfonated calix[6] arene functionalized grapheme, ACS Appl. Mater. Interfaces 7 (2015) 26557–26565.
[19] L. Yang, X.G. Xie, L. Cai, X. Ran, Y.C. Li, T.P. Yin, H. Zhao, C.P. Li, P-sulfonated calix[8]arene functionalized grapheme as a "turn on" fluorescent sensing platform for aconitine determination, Biosens. Bioelectron. 82 (2016) 146–154.
[20] Z.M. Liu, Y. Yang, H. Wang, Y.L. Liu, G.L. Shen, R.Q. Yu, A hydrogen peroxide biosensor based on nano-Au/PAMAM dendrimer/cystamine modified gold electrode, Sens. Actuators B Chem. 106 (2005) 394–400.
[21] L. Yang, H. Zhao, C.P. Li, S.M. Fan, B.C. Li, Dual β-cyclodextrin functionalized Au@SiC nanohybrids for the electrochemical determination of tadalafil in the presence of acetonitrile, Biosens. Bioelectron. 99 (2015) 126–130.
[22] Web reference 4: The Diagnosis and Treatment Protocol of COVID-19, http://www.chinacdc.cn/jkzt/crb/xcrxjb/202002/t20200205_212257.html(accessed 2020/02/05).
[23] C. Xie, L. Jiang, G. Huang, H. Pu, B. Gong, H. Lin, S. Ma, X. Chen, B. Long, G. Si, H. Yu, L. Jiang, X. Yang, Y. Shi, Z. Yang, Comparison of different samples for 2019 novel coronavirus detection by nucleic acid amplification tests, Int. J. Infect. Dis. 93 (2020) 264–267.
[24] Y. Pan, D. Zhang, P. Yang, L.L.M. Poon, Q. Wang, Viral load of SARS-CoV-2 in clinical samples, Lancet Infect. Dis. 20 (2020) 411–412.
[25] F.T. Yu, L.T. Yan, N. Wang, S.Y. Yang, L.H. Wang, Y.X. Tang, G.J. Gao, S. Wang, C. J. Ma, R.M. Xie, F. Wang, C.N. Tan, L.X. Zhu, Y. Guo, F.J. Zhang, Quantitative detection and viral load analysis of SARS-CoV-2 in infected patients, Clin. Infect. Dis. 71 (2020) 793–798.
[26] Web reference 5: Interim Guidelines for Collecting, Handling, and Testing Clinical Specimens from Persons under Investigation (PUIs) for Coronavirus Disease 2019 (COVID-19), https://www.cdc.gov/coronavirus/2019-nCoV/lab/guidelines-clinical-specimens.html (accessed 2020/05/22).
[27] C.T. Wang, Z.P. Liu, Z.X. Chen, X. Huang, M.Y. Xu, T.F. He, Z.H. Zhang, The establishment of reference sequence of SARS-CoV-2 and variation analysis, J. Med. Virol. 92 (2020) 667–674.
[28] V.M. Corman, O. Landt, M. Kaiser, R. Molenkamp, A. Meijer, D.K.W. Chu, T. Bleicker, S. Brünink, J. Schneider, M.L. Schmidt, D.G.J.C. Mulders, B. L. Haagmans, B. Van der Veer, S.V.D. Brink, L. Wijsman, G. Goderski, J.L. Romette, J. Ellis, M. Zambon, M. Peiris, H. Goossens, C. Reusken, M.P.M. Koopmans, C. Drosten, Detection of 2019 novel coronavirus (2019-nCoV) by real-time RT-PCR, Euro Surveill. 25 (2020), 2000045.
[29] D.K.W. Chu, Y. Pan, S.M.S. Cheng, K.P.Y. Hui, P. Krishnan, Y.Z. Liu, D.Y.M. Ng, C. K.C. Wang, P. Yang, Q.Y. Wang, M. Peiris, L.L.M. Poon, Molecular diagnosis of a novel coronavirus (2019-nCoV) causing an outbreak of pneumonia, Clin. Chem. 66 (2020) 549–555.

[30] J.P. Broughton, X.D. Deng, G.X. Yu, C.L. Fasching, V. Servellita, J. Singh, X. Miao, J.A. Streithorst, A. Granados, A.S. Gonzalez, K. Zorn, A. Gopez, E. Hsu, W. Gu, S. Miller, C.Y. Pan, H. Guevara, D.A. Wadford, J.S. Chen, C.Y. Chiu, CRISPR-Cas12-based detection of SARS-CoV-2, Nat. Biotechnol. 38 (2020) 870–874, https://doi.org/10.1038/s41587-020-0513-4.

[31] K. Uhteg, J. Jarrett, M. Richards, C. Howard, E. Morehead, M. Geahr, L. Gluck, A. Hanlon, B. Ellis, H. Kaur, P. Simner, K.C. Carroll, H.H. Mostafa, Comparing the analytical performance of three SARS-CoV-2 molecular diagnostic assays, J. Clin. Virol. 127 (2020), 104384.

[32] A. Bordi, E. Piralla, F. Lalle, F. Giardina, M. Colavita, G. Tallarita, F. Sberna, S. Novazzi, C. Meschi Castilletti, A. Brisci, G. Minnucci, V. Tettamanzi, F. Baldanti, M.R. Capobianchi, Rapid and sensitive detection of SARS-CoV-2 RNA using the Simplexa™ COVID-19 direct assay, J. Clin. Virol. 128 (2020), 104416.

[33] R. Lu, X.M. Wu, Z.Z. Wan, Y.W. Li, X. Jin, C.Y. Zhang, A novel reverse transcription Loop-mediated isothermal amplification method for rapid detection of SARS-CoV-2, Int. J. Mol. Sci. 21 (2020) 2826.

[34] B. Visseaux, Q.L. Hingrat, G. Collin, D. Bouzid, S. Lebourgeois, D.L. Pluart, L. Deconinck, F.X. Lescure, J.C. Lucet, L. Bouadma, J.F. Timsit, D. Descamps, Y. E. Yazdanpanah Casalino, N.H. Fidouh, Emergency Department Influenza Study Group, Valuation of the QIAstat-Dx respiratory SARS-CoV-2 panel, the first rapid multiplex PCR commercial assay for SARS-CoV-2 detection, J. Clin. Microbiol. 58 (2020) e00630-20.

Hui Zhao is a professor in Yunnan University, Kunming, China. She received her Ph. D. degree in Biochemistry from Yamaguchi University, Japan. Her current research interests are biosensor and functional gene.

Feng Liu is currently pursuing Dr. degree in Yunnan University, Kunming, China. Her research interests are mainly focused on electrochemical nucleic acid sensor.

Wei Xie is currently pursuing master's degree in Yunnan University, Kunming, China. Her research interests are mainly focused on electrochemical sensors based on supramolecular recognition.

Tai-Cheng Zhou is a researcher in the Central Lab, Liver Disease Research Center, the Second People's Hospital of Yunnan Province, who's research interests are mainly focused on genetic diseases.

Jun Ouyang is currently pursuing master's degree in Yunnan University, Kunming, China. His research interests are mainly focused on cancer genes.

Lian Jin is currently pursuing master's degree in Yunnan University, Kunming, China. Her research interests are mainly focused on cancer genes.

Hui Li is a researcher in the Central Lab, Liver Disease Research Center, the Second People's Hospital of Yunnan Province, whose research interests are mainly focused on genetic diseases.

Chun-Yan Zhao is a researcher in the Central Lab, Liver Disease Research Center, the Second People's Hospital of Yunnan Province, whose research interests are mainly focused on genetic diseases.

Liang Zhang is a researcher in the Central Lab, Liver Disease Research Center, the Second People's Hospital of Yunnan Province, whose research interests are mainly focused on biomarkers in genetic diseases.

Jia Wei is the director of the Second People's Hospital of Yunnan Province, whose research interests are mainly focused on the diagnosis of infectious diseases.

Ya-Ping Zhang is a professor in Yunnan University, Kunming, China. He received his Ph. D. degree in genetics from Kunming Institute of Zoology, Chinese Academy of Sciences, China. His current research interests are molecular evolution and genome biodiversity.

Can-Peng Li received his MS and Ph.D. degree from Kagoshima University, Japan, in 2002 and 2005. Since 2007, he has been working at Yunnan University as a professor. His research interests are focused on fluorescence/electrochemical sensors, biosensors, and functional food.